

## High-pressure x-ray absorption study of InSe

J. Pellicer-Porres,\* A. Segura, and V. Muñoz

*Institut de Ciència dels Materials, Universitat de València, C/Dr. Moliner 50, Edifici Investigació 1.10, E-46100 Burjassot (València), Spain*

A. San Miguel

*Département de Physique des Matériaux, Bâtiment 203, Université Lyon I, 43 Boulevard du 11 Novembre 1918, F-69622 Villeurbanne, France*

(Received 16 December 1998)

The III-VI layered semiconductor InSe has been studied by high-pressure single crystal x-ray absorption spectroscopy up to a maximum pressure of 14 GPa. The In-Se distance has been measured in both the low-pressure layered phase and the high-pressure NaCl phase. The bond compressibility in the layered phase is lower than the “a” crystallographic parameter compressibility, which implies an increase of the angle between the In-Se bond and the layer plane. Under plausible hypothesis, a description of the evolution of the whole structure with pressure is given. In particular, the intralayer distance is observed to increase with increasing pressure. A plausible precursor defect and a simple mechanism for the transition are also presented. The conclusions can be readily translated to other III-VI layered semiconductors. [S0163-1829(99)07729-2]

### I. INTRODUCTION

Layered materials constitute a challenging case for the development of models that could be able to simultaneously describe electronic interactions of very different nature. Under high pressure, the strength of intra- and interlayer interactions evolve in a drastically different manner, and the evolution of the associated physical properties constitutes a strong test of validity for theoretical models. In the family of layered III-VI materials, the covalent layers are separated by the so-called van der Waals gap, with weak interactions of van der Waals type between the layers. Consequently, this gap follows a pressure evolution considerably different from the evolution of any characteristic distance inside the layers. Besides the fundamental interest of this type of materials, many technical applications have been proposed in nonlinear optics,<sup>1,2</sup> the development of solar cells<sup>3,4</sup> or as candidates for solid state batteries.<sup>5</sup>

InSe is a representative member of the III-VI layered family (GaS, GaSe, GaTe, and InSe).<sup>6</sup> With the exception of GaTe,<sup>7</sup> the intralayer stacking of these compounds can be described by a  $X-Y-Y-X$  scheme ( $X$  being the anion and  $Y$  the cation). In turn, different interlayer stacking patterns have been observed, labeled  $\beta$ ,  $\varepsilon$ ,  $\gamma$ . Even if the  $\beta$  and the  $\varepsilon$  forms have been proposed for InSe,<sup>6</sup> single crystals seem to follow the  $\gamma$  interlayer scheme<sup>8,9</sup> (space group  $R3m$ ), namely an  $ABCABC\dots$  stacking (Fig. 1). Each atomic plane ( $X=Se$  or  $Y=In$ ) can be seen as a (111) plane in a conventional zincblende structure, the  $XY$  sublayers being constituted by hexagonal cycles with chairlike deformation. The  $XY$  and the  $YX$  sublayers are connected by In-In bonds perpendicular to the layers. The whole gives rise to quasitetrahedral coordination for the In atoms (three Se and one In) and threefold coordination for Se with In atoms. On average, the Hume-Rothery rule is preserved. The  $ABCABC$  interlayer stacking is carried out through successive  $\mathbf{t}=(\mathbf{a}+\mathbf{b})/3$  translations of each layer (where  $\bar{a}$  and  $\bar{b}$  are the basis vectors from the hexagonal description).

The properties of InSe at ambient pressure have been extensively studied. Under pressure, optical absorption,<sup>10-12</sup> photoluminescence,<sup>13</sup> low frequency dielectric constant,<sup>14</sup> optical reflectivity,<sup>15</sup> transport,<sup>16</sup> Raman spectroscopy,<sup>15,17,18</sup> and x-ray diffraction<sup>15,19</sup> (XRD) studies have been performed. At ambient temperature, the  $\gamma$  modification is stable up to 10.3(5) GPa, where a first order transition with a volume variation of 14.8% towards a NaCl structure is observed.<sup>15</sup> The rocksalt modification presents a metallic character (in ambient conditions  $\gamma$ -InSe has a direct gap of 1.35 eV) and remains stable up to at least 30 GPa. The compressibility of the low-pressure phase is highly anisotropic, showing on the one hand a linear and rather moderate compressibility of the  $a$  axis and on the other hand a marked

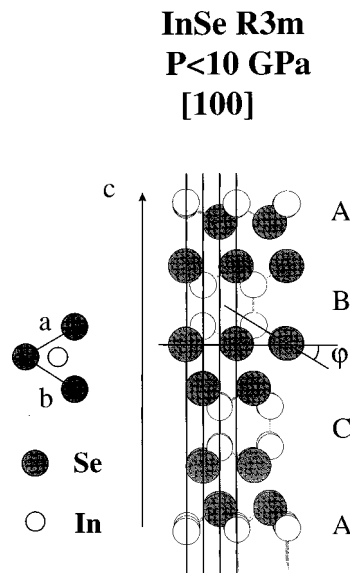


FIG. 1. InSe low-pressure modification (space group  $R3m$ ). The layered structure is described in the text. Black and white atoms correspond to Se and In atoms, respectively.  $a$ ,  $b$ , and  $c$  are the basis lattice vectors from the hexagonal description of the structure.

nonlinear and high compressibility along the  $c$  axis. At about 7 GPa progressive and irreversible appearance of dislocation related dark lines is manifested by direct optical observations in single crystals,<sup>20</sup> but no trace of phase transition is evidenced by XRD. Nevertheless, the appearance of a phonon mode near 7 GPa (Ref. 17) suggests a structural instability of InSe below the transition pressure to the metallic phase. Furthermore, near 4 GPa and at 250 °C, a stabilization of a monoclinic modified InS-type nonlayered structure has been obtained.<sup>18,19</sup>

An essential problem in the description of the physical properties at high pressure in III-VI layered compounds is the lack of information concerning the pressure evolution of the atomic arrangement inside the unit cell [up to our knowledge the experimental determination of the atomic positions inside the unit cell has only been possible in GaS (Ref. 21)]. This implies the introduction of additional assumptions in models to compute electronic band structure under pressure<sup>22</sup> and is a fundamental limitation for total energy calculations. This problem can be attributed to experimental difficulties introduced by the layered character of the material that on the one side makes very difficult to obtain a pure single-crystalline sample (the presence of stacking defects or twinned planes is almost unavoidable) and on the other side introduces preferential orientation in powdered samples. In InSe, the only reported XRD study<sup>15</sup> could not give any indication on the pressure evolution of the atomic positions. X-ray absorption spectroscopy<sup>23</sup> (XAS) is a very powerful technique that provides information on the local structure as a function of pressure and is consequently an excellent complement for XRD studies at high pressure.<sup>24</sup> The combination of the two techniques has already been successful in the determination of the full structure of high-pressure structures of materials.<sup>25</sup>

We have performed high-pressure single crystal x-ray absorption spectroscopy at the Se  $K$ -edge on InSe up to 14 GPa in order to obtain maximal information of the pressure evolution of the local structure.

## II. EXPERIMENT

High quality InSe crystals were prepared by the Bridgman method from a nonstoichiometric melt of  $\text{In}_{1.05}\text{Se}_{0.95}$ . Samples were cleaved from the ingots with a razor blade and cut into parallelepipeds with typical dimensions of  $100 \times 150 \times 30 \mu\text{m}^3$ . A wide angle aperture membrane diamond anvil cell<sup>26</sup> was used as pressure generator. The diamonds were of the Drukker standard type, with culet size of 0.5 mm. The single crystal sample was placed in a 250  $\mu\text{m}$  diameter hole drilled in an Inconel gasket. Silicon oil was used as pressure transmitting medium and the pressure was measured *in situ* using the linear ruby fluorescence scale.<sup>27</sup>

The x-ray absorption experiments were carried out at the ID24 energy dispersive x-ray absorption station of the European Synchrotron Radiation Facility (Grenoble, France).<sup>28</sup> A profiled curved Si(111) monochromator<sup>29</sup> focused the beam to a spot of approximately 50  $\mu\text{m}$  in the horizontal direction. In the vertical direction the beam was only slit to 100  $\mu\text{m}$ . Details on the principle of energy dispersive x-ray absorption data collection can be found elsewhere.<sup>30</sup> An essential experimental aspect of XAS experiments at high pressure is the

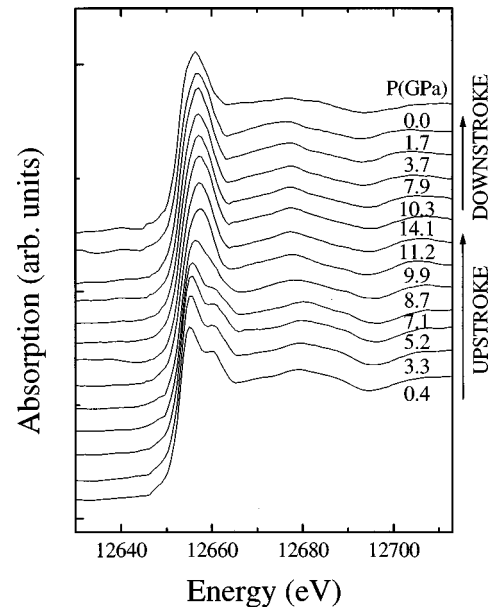


FIG. 2. XANES spectra of InSe at the Se  $K$  edge at different pressures for one of the orientations of the cell.

presence of glitches in the XAS spectra originated by XRD by the diamond single crystals. The pressure cell is oriented with respect to the polychromatic x-ray beam in order to remove these glitches from the widest spectral domain around the x-ray absorption edge. This operation takes advantage of the real time visualization of the XAS spectra thanks to the x-ray parallel collection characteristic of the energy dispersive setup. In our experiment, the sample itself being a single crystal, additional XRD glitches come into the spectra and make the cell orientation process even harder. To give us the best chances of finding a good orientation of the cell plus sample system: (i) a wide angular aperture diamond anvil cell was used, (ii) the sample was immobilized inside the cell by using a relatively viscous pressure transmitting media. Nevertheless it was not possible to obtain an orientation where the XANES (x-ray absorption near edge structure) part and the EXAFS (extended x-ray absorption fine structure) part of the spectra could be simultaneously collected and two different orientations of the cell were needed for each pressure measurement: the first one for the XANES part and the second for the EXAFS one, which will be discussed in the next section.

## III. RESULTS AND DISCUSSION

### A. XANES

The XANES part of the x-ray absorption spectra is depicted in Fig. 2 for some significant pressure values and corresponding to one of the orientations of the cell with respect to the x-ray beam. In contrast with the EXAFS part of a XAS spectrum, the XANES one involves multiple scattering processes and is consequently sensitive to medium-range order (up to 15 Å around the absorbing atom in some cases). During the upstroke process, significant changes of the XANES part start to be observed from 7.1 GPa. At this pressure, the doublet structure of the white line starts to smear giving rise to a singlet structure that is already well defined from 9.9

TABLE I. Proportion of local mixing in the XANES part of the spectra during the phase transition. As characteristic from the low- and high-pressure phases we have taken the spectra at 5.2 and 11.2 GPa, respectively.

Experimental spectra	% of spectrum at 5.2 GPa	% of spectrum at 11.2 GPa
Spectrum at 7.1 GPa	$88 \pm 5$	$12 \pm 5$
Spectrum at 8.7 GPa	$47 \pm 5$	$53 \pm 5$
Spectrum at 9.9 GPa	$5 \pm 5$	$95 \pm 5$

GPa. The first broad structure after the white line shows equally a different scheme from this last pressure value. The whole evidences a structural phase transformation. The change from a doublet structure of the white line to the singlet one have been observed in the pressure induced phase transformation of many tetrahedral semiconductors to higher coordination schemes (five- or sixfold coordination). Therefore, XANES suggests an increase in the coordination number. The XANES scheme of the high-pressure phase is preserved up to the highest pressure attained (14.1 GPa) and is kept during the downstroke process up to approximately 1.7 GPa, indicating that the high pressure local structure is maintained up to this pressure. Nevertheless, it is not recovered at ambient conditions as can be seen by the shape of the top spectrum in Fig. 2. In fact, totally new XANES resonances appear, exhibiting a net broadening of the structures. This is in agreement with the irreversible feature of the transition and the amorphous character of the recovered sample that has been observed by XRD.<sup>15</sup> We also observe that the singlet high-pressure scheme of the white line is kept in the recovered sample, suggesting that the amorphous phase is not based on tetrahedral units.

The XANES part can be used to determine the proportion of local mixing spectra taken at 7.1, 8.7, and 9.9 GPa. We have tried to reproduce these spectra with proper weighting of characteristic normalized spectra from the low (spectrum at 5.2 GPa) and high-pressure phases (spectrum at 11.2 GPa). The results have been successful and are presented in Table I. We conclude that a progressive change in the coordination of the Se atoms is produced.

### B. EXAFS

The EXAFS oscillations were extracted from the spectra obtained in a second orientation of the cell with respect to the x-ray beam. XRD glitches were limiting the useful spectral domain to 250 eV after the edge. The pair-pseudo-distribution function (PPDF) is obtained by Fourier transformation of the EXAFS signal in a  $k$  domain between 2.8 and 7.8  $\text{\AA}^{-1}$  and using a Bessel based ( $\tau=2.5$ ) apodization window. It is shown in Fig. 3 for different pressures. The contribution of the first neighbor shell to the PPDF corresponds to the doublet structure observed between approximately 1 and 3  $\text{\AA}$ . This doublet is characteristic of the presence of scattering atoms of high atomic number.<sup>31</sup> The most noticeable fact is the sudden shift of the doublet to higher distance values between 9.9 and 11.2 GPa, indicating a structural rearrangement at a pressure of  $10.5 \pm 1.0$  GPa, with a sudden increase of interatomic distances. As a consequence of the

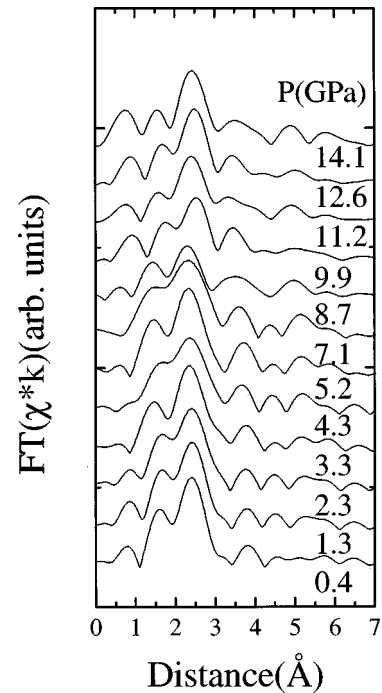


FIG. 3. Pair-pseudo-distribution function (PPDF) obtained by Fourier transformation of the EXAFS signal. The contribution of the first neighbor shell (Se-In) to the PPDF corresponds to the doublet structure observed between approximately 1 and 3  $\text{\AA}$ .

limited range of  $k$  values available in dispersive EXAFS and also due to the close sequence in neighbor distances present in InSe, only the first neighbor shell is clearly observable in the PPDF. The EXAFS fit of the filtered part of the PPDF corresponding to the first neighbor shell provides quantitative information on the local structure.

The spectrum taken at ambient conditions was used to extract the EXAFS phases and amplitudes corresponding to the Se-In backscattering process, using the known structural data.<sup>8,9</sup> This allows to follow the pressure variation of the structural parameters of the first coordination shell. In Fig. 4 is shown the evolution of the intralayer first neighbor Se-In

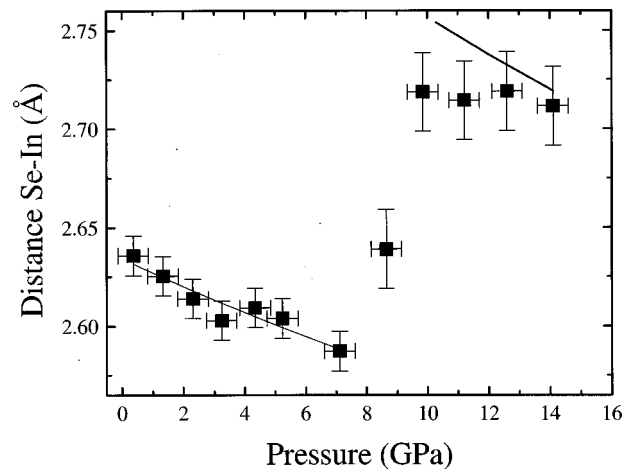


FIG. 4. Evolution of the intralayer first neighbor Se-In distance obtained from the EXAFS fit. Up to 7.1 GPa it follows a monotonic compression that has been fitted to a Murnaghan equation of state [Eq. (1)], resulting in  $B_0 = 116 \pm 20$  GPa with  $B'_0 = 5$ .

distance obtained from the EXAFS fit. This distance follows a monotonous compression up to 7.1 GPa that has been fitted to a first order Murnaghan equation of state,<sup>32</sup>

$$d_{\text{SeIn}} = d_{\text{SeIn}0} \left( 1 + \frac{B'_0}{B_0} P \right)^{-1/3B'_0}, \quad (1)$$

where  $d_{\text{SeIn}0}$  is the Se-In distance at ambient conditions (2.634 Å),  $B_0$  is the isothermal bulk modulus at zero pressure, and  $B'_0$  its pressure derivative. The data dispersion avoids to obtain  $B_0$  and  $B'_0$  simultaneously. In order to obtain comparative values with other III-VI layered compounds, we have fixed, as in the case of GaSe,<sup>33</sup>  $B'_0$  to a value of 5, resulting in a bulk modulus of  $B_0 = 116 \pm 20$  GPa. This value is very close to the ones obtained for GaSe (Ref. 33) (110 GPa) and GaTe (Ref. 34) ( $124 \pm 6$  GPa).

### C. Structural changes induced by pressure

The variation of the Se-In distance with pressure is much slower than the variation found by x-ray studies for the  $\mathbf{a}$  lattice vector ( $B_{0a} = 44$  GPa,  $B'_{0a} = 5$ ). To make both values in agreement the angle between the Se planes and the Se-In bond ( $\varphi$ ) must change. At ambient conditions its value is  $\varphi = 28.7^\circ$ . Supposing that the trigonal symmetry of the Se atoms in the layer plane and the perpendicularity of the In-In bonds with respect to the Se planes is maintained, the Se-In distance and the modulus of the  $\mathbf{a}$  lattice vector are related by

$$\frac{a}{2} = d_{\text{SeIn}} \cos(\varphi) \cos 30^\circ. \quad (2)$$

Then the  $\varphi$  value at 10 GPa is  $31.4^\circ$ .

As mentioned in the Introduction, the knowledge of the evolution of the whole structure under pressure would be an invaluable aid to test the evolution of theoretical models, as for example band structure models. Up to now, in layered materials this has been possible only in GaS (Ref. 21) through XRD measurements, and this because of its high symmetry ( $\beta$  polytype,  $P6_3/mmc$ ) and the presence of only two nonequivalent atoms in the unit cell. In that experiment it was shown that the Ga-Ga and Ga-S distances follow the same relative behavior under pressure. It is then logical to assume that the In-In and Se-In distances vary in the same way under pressure. The In-In bond in InSe and the Ga-Ga distance in GaS then follow a similar variation. With this additional presumption we can follow the evolution of the whole structure with pressure. Let us call  $z_{\text{In}1}, z_{\text{In}2}, z_{\text{Se}1}, z_{\text{Se}2}$  the  $z$  fractional coordinates in the hexagonal description of the structure and  $d_i$  the interlayer distance. Then, we have

$$z_{\text{In}1} = 0, \quad (3a)$$

$$z_{\text{In}2} = \frac{d_{\text{In-In}}}{c}, \quad (3b)$$

$$z_{\text{Se}1} = \frac{1}{c} (c - d_i - d_{\text{SeIn}} \sin(\varphi)), \quad (3c)$$

$$z_{\text{Se}2} = \frac{1}{c} (c - d_i - 3d_{\text{SeIn}} \sin(\varphi) - d_{\text{In-In}}), \quad (3d)$$

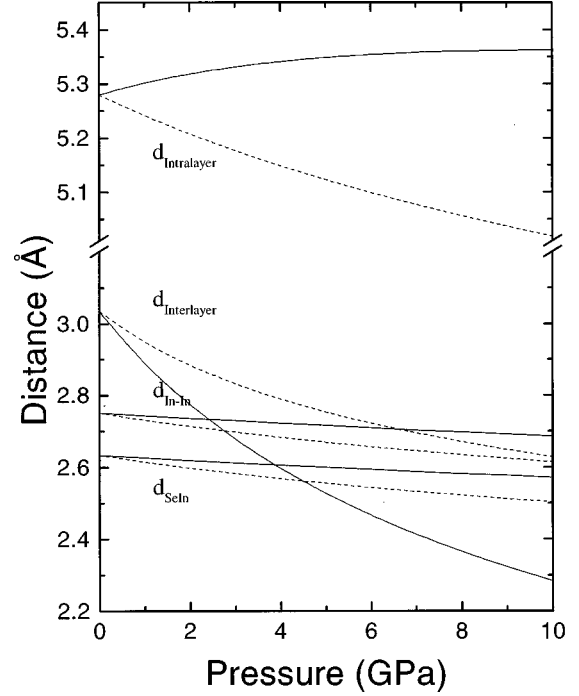


FIG. 5. Evolution under pressure of the intralayer, interlayer, In-In, and Se-In distances under two hypothesis: (a) the In-In bond length variation is assumed to be the same as the Se-In (continuous lines); (b) the layers are supposed to be isotropic, i.e., its compressibility along the  $c$  axis is taken from the compressibility along the  $a$  axis (dashed lines).

$$d_i = \frac{c}{3} - d_{\text{InIn}} - 2d_{\text{SeIn}} \sin(\varphi). \quad (3e)$$

The Se-In, In-In, interlayer and intralayer distances calculated from the above formulas are depicted in Fig. 5 as continuous lines. It is remarkable the slight increase in the intralayer distance with pressure. The augmentation is due to the fact that the  $2d_{\text{SeIn}} \sin(\varphi)$  increment is not compensated by the diminution in  $d_{\text{InIn}}$ . In previous works<sup>10,39</sup> the layer compressibility was supposed to be isotropic. The  $d_{\text{InIn}}$ , intralayer and interlayer distances calculated under this hypothesis are presented in Fig. 5 as dashed lines. An important consequence of Fig. 5 is that the intralayer and interlayer deformation potentials for the direct and indirect gaps in InSe and GaSe should be recalculated.<sup>35</sup>

The pseudo Debye-Waller (DW) factors obtained in the EXAFS analysis are presented in Fig. 6. The DW gives an idea of the degree of both dynamic and static disorder. Combining the Einstein approximation with Raman-scattering data under pressure we can evaluate an approximation for the harmonic dynamic part of the DW.<sup>36-38</sup> In InSe this calculation results in a diminution in the DW of the order of  $10^{-4} \text{ \AA}^2$ , far away from the observed experimental increase, that can therefore undoubtedly be attributed to a considerable increase of the static disorder. The static disorder suffers a drastic increase from 6 GPa.

Although the rough shape of the PPDF for the high-pressure phase seems to be achieved at 9.9 GPa, the low amplitude of the PPDF peaks shows that the disorder is considerably high at this pressure, and it does not attain a value comparable to the amplitude of the low-pressure phase even



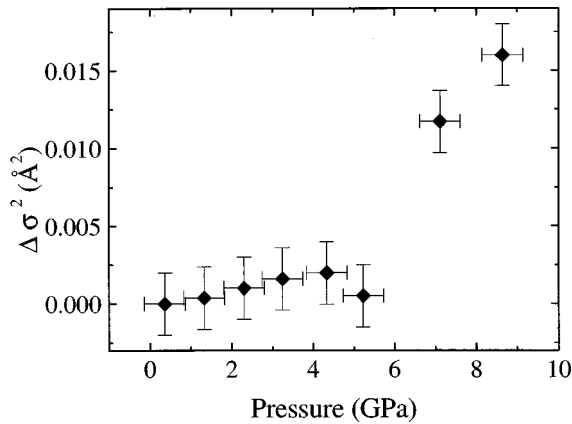


FIG. 6. EXAFS pseudo-Debye-Waller factor variation under pressure obtained in the EXAFS analysis.

at the highest pressure measured, 14.1 GPa. Nevertheless, the EXAFS analysis shows that, from 12.6 GPa on, the distance Se-In varies following the equation obtained by XRD (Ref. 15) for the rocksalt high-pressure phase (if we take into account the errors coming both from the experience and from the transferability to the high-pressure phase of the phases and amplitudes obtained from the low-pressure phase). The rocksalt high-pressure phase was possibly crystallized at the highest pressure attained, but the PPDF indicates that it is not fully crystallized. In the downstroke process, no satisfactory fit has been obtained.

#### D. Mechanism of the transition and its possible precursor defects

We are now in situation to discuss the mechanism of the transition and its possible precursor defects. The most sensitive techniques to the apparition of defects in semiconductors are transport and optical measurements. In particular, in InSe, due to the existence of a localized impurity level associated with a subsidiary minimum in the conduction band, the carrier concentration is shown to reversibly decrease under pressure up to 4 GPa approximately,<sup>16</sup> reaching a value of  $10^{15} \text{ cm}^{-3}$  (in tin doped samples with  $10^{17} \text{ electrons/cm}^{-3}$  at ambient pressure), that can therefore be considered as the sensibility limit for carrier measurements in InSe at 4 GPa. Any further nonreversible increase above 4 GPa is attributed to the formation of donor defects. At 10 GPa the number of carriers is  $10^{21} \text{ cm}^{-3}$ . If we suppose a defect per carrier, this implies a proportion of defects just before the transition in the order of 1 defect per 10 unit cells. In optical absorption experiments,<sup>10</sup> the crystal turns opaque at a pressure near 6 GPa. At about 7 GPa progressive and irreversible appearance of dislocations is manifested by direct optical observations in single crystals.<sup>20</sup> In Raman experiments,<sup>17</sup> for pressures higher than 7 GPa, the spectra show an additional feature (respect to the low-pressure spectra) that was associated with a local vibrational mode related to structural defects. In our EXAFS experiment, the DW indicates a progressive increase in the static disorder, with a more important augmentation near 6 GPa. Finally, the analysis of the XANES shows that at 7.1 GPa approximately 12% of the Se atoms have changed their configuration. Summarizing, all the methods indicate a

continuous formation of defects, which is evidenced at different pressures depending on the sensitivity of the method.

A possible candidate for the defect is one where an In atom breaks its bond with the other intralayer In atom and jumps to the interlayer space, where it has octahedral coordination.<sup>16</sup> This candidate is convincing for several reasons. First of all, the Se-In-In-Se plane sequence should change to a Se-In-Se-In sequence in the phase transition to a NaCl type structure.

Second, Raman measurements bring to evidence the progressive weakening of the cation-cation bond in III-VI layered semiconductors. For example, GaSe has two Se-Ga-Ga-Se structural units per unit cell. In this compound, the  $E''^{(2)}$  and  $E''^{(1)}$  phonon modes are Davydov conjugate partners where the Se-Ga sublayers vibrate against each other. In the  $E''^{(2)}$  and  $E''^{(1)}$  modes, the Se-Ga-Ga-Se layers vibrate in phase and out of phase respectively. The frequency of the  $E''^{(1)}$  mode is dominated by the Ga-Ga bond bending force whereas the frequency of the  $E''^{(2)}$  mode is dominated both by the intralayer and interlayer bond. The low intensity of the Raman peak associated with the  $E''^{(1)}$  mode makes impossible its detection under pressure. The  $E''^{(2)}$  frequency evolution under pressure shows only a slight augmentation<sup>39</sup> ( $0.83 \text{ cm}^{-1}/\text{GPa}$ ). As the force constant associated with the interlayer bond is known to increase under pressure, this is interpreted as a weakening of the intralayer bond.<sup>39,40</sup> What is more, using a coupled oscillator model for the Davydov conjugate modes,<sup>40</sup> one can estimate the frequency variation of the  $E''^{(1)}$  mode, resulting in a softening of  $-2.9 \times 10^{-2} \text{ GPa}^{-1}$ . In InSe there is only one Se-In-In-Se structural unit per unit cell. InSe and GaSe phonon dispersion curves in the  $\Gamma Z$  direction are related by a twofolding. The  $E''^{(1)}$  mode in the  $\Gamma$  point in GaSe is equivalent in InSe to the  $E^{(2)}$  mode in the edge border of the Brillouin zone. This mode is not accessible through first order Raman measurements. So, experimentally it is not possible to see directly the softening of the mode associated with the In-In bond. But as in GaSe, the  $E^{(2)}$  force constant is dominated both by the intralayer and interlayer bonds and the frequency evolution in pressure of this phonon shows an even lower increase<sup>17</sup> ( $0.68 \text{ cm}^{-1}/\text{GPa}$ ). We can conclude that the In-In bond weakens under pressure.

The proposed defect formation mechanism above mentioned would also justify the apparition of donor levels observed in transport measurements. If an In-In bond is broken and one In jumps to the interlayer space, two cation dangling bonds remain. In partly ionic compounds, cation dangling bonds occur in anion vacancies and have donor character.

We have also observed a progressive change in the stiffness properties of samples submitted to pressure cycles and then recovered. They lose in part their layer character, to the point that samples pressurized above 6 GPa are susceptible to be polished. In our scheme, the cation situated in the interlayer space would be responsible for the partial loss of the layered character.

Finally, this candidate for the defect would explain the features observed in the XANES and in the EXAFS part of our experiment. The change in coordination showed by the XANES from 7.1 GPa is readily understood when considering the differences in coordination of the Se sites before and after the jump. We have analyzed the first neighbor shell

contribution to the PPDF at 8.7 GPa employing two distances and assigning the same number of neighbors to both of them as suggested by Table I. The fitting gives  $d_1 = 2.58 \pm 0.02$  and  $d_2 = 2.79 \pm 0.02$  Å, suggesting that when the In atom occupies the octahedral site there is a reorganization of distances around it to match the Se-In distance of the rock-salt structure. Then it seems logical to think that the stress created by such a distortion is responsible for the high number of dislocations apparent in direct optical measurements. The dislocations themselves would increment the stresses in the sample and favor the formation of more defects, specially in their surroundings. The static disorder observed in the DW is then assigned to the difference between both distances. Its increment is interpreted as due to the augmentation of the number of Se atoms in octahedral configuration. The PPDF evolution near the transition can be interpreted in the same way, as the sum of two contributions, one of them (octahedral contribution) considerably smeared due to the dispersion in Se-In distances in the octahedral site. At 9.9 GPa the PPDF has such low amplitude because of the small proportion of “ordered” Se sites. At this moment, the proportion of broken In-In bonds is very high (1 per 10 unit cells, as estimated by transport measurements), the structure is destabilized and a reorganization of the whole structure occurs. The left In-In bonds are broken and half of the In atoms of each layer jump to the interlayer space. Then the remaining In-Se sublayer suffers a translation of magnitude  $\mathbf{t}$  as indicated in Fig. 7. At the same time the intralayer and interlayer thicknesses are diminished and augmented respectively to adequate the Se-In distance to the value of the rock-salt structure (2.74 Å). With only these small changes the ABC stacking sequence of the NaCl structure is reproduced. After the transition, the PPDF at 11.2 GPa shows an increment of amplitude associated with a diminution in the dispersion of the Se-In distances, that now show its change with respect to the low-pressure phase. Anyway, as commented above, the amplitude does not attain values comparable to the low-pressure phase because it is not fully crystallized.

Finally, it is worth noting that this is a simple way to describe the transition. The precise way in which the In atoms jump (if all the In atoms of a layer jump in the same sense or how the jumps are favored by the presence of dislocations, for example) should be elucidated by theoretical calculations.

#### IV. CONCLUSIONS

InSe has been studied by high-pressure single crystal x-ray absorption spectroscopy up to a maximum pressure of 14 GPa. XANES shows that between 7.1 and 9.9 GPa a nonreversible change in the Se coordination occurs. This is interpreted as a consequence of a progressive defect formation consisting in the jump of In atoms to the interlayer space, consistently with transport, optical, Raman, XRD, and direct observation experiments. The PPDF shows that at  $10.5 \pm 1$  GPa the Se and In atoms are ordered following the rock-salt structure pattern, but full crystallization is not observed before 12.6 GPa.

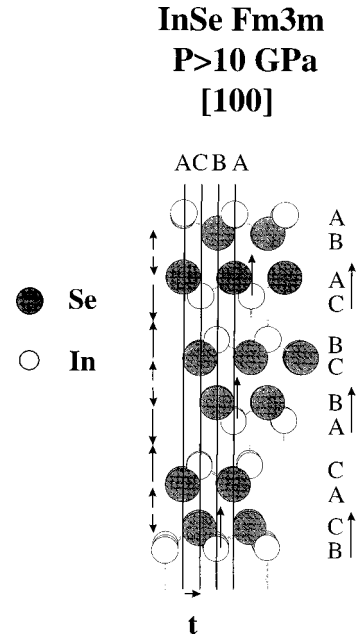


FIG. 7. One possible way to accomplish the phase transition from the low-pressure layered phase to the high-pressure modification (rock-salt structure, space group  $Fm\bar{3}m$ ). As shown in the figure, an In-In bond is broken, one In atom jumps to the octahedral site in the interlayer space, two sublayers (as sketched in the figure) are translated a vector  $\mathbf{t} = (\mathbf{a} + \mathbf{b})/3$ , and finally the interlayer and intralayer distances are adjusted to match the new values in the rock-salt structure.

The EXAFS fit of the filtered part of the PPDF corresponding to the first neighbor shell is used to extract information about the Se-In bond length and DW variation under pressure. The DW increment under pressure is interpreted as due to the increase in static disorder associated with the progressive apparition of defects. From the monotonous compression of the Se-In distance up to 7.1 GPa we get  $B_0 = 116 \pm 20$  GPa with  $B_0 = 5$ . Assuming that the trigonal symmetry of the Se atoms in the layer plane and the perpendicularity of the In-In bonds with respect to the Se planes is maintained and that the In-In bond length variation under pressure is proportional to the Se-In variation, we can obtain an evolution of the whole structure under pressure. In particular, calculations give an increase in the angle between the Se planes and the Se-In bond (from  $28.5^\circ$  at ambient conditions to  $31.4^\circ$  at 10 GPa). This augmentation is finally responsible for the obtained slight increase of the intralayer distance. Our results do not confirm previous works, where the layers were considered as isotropic and where, accordingly, the intralayer distance diminished with pressure. These results could be fundamental in theoretical calculations in InSe and can be readily translated to other III-VI layered semiconductors.

#### ACKNOWLEDGMENTS

This work was supported by the Spanish government CICYT under Grant No. MAT95-0391.

- \* Author to whom correspondence should be addressed. FAX: (34) 96 3983146; electronic address: Julio.Pellicer@uv.es
- <sup>1</sup>W. C. Eckhoff, R. S. Putnam, S. Wang, R. F. Curl, and F. K. Tittel, *Appl. Phys. B: Lasers Opt.* **B63**, 437 (1996).
- <sup>2</sup>M. A. Hernández, J. F. Sánchez, M. V. Andrés, A. Segura, and V. Muñoz, *Opt. Pura Apl.* **26**, 152 (1993).
- <sup>3</sup>A. Segura, J. M. Besson, A. Chevy, and M. S. Martin, *Nuovo Cimento B* **38**, 345 (1977).
- <sup>4</sup>O. Lang, R. Rudolph, A. Klein, C. Pettenkofer, W. Jaegermann, J. Sánchez, A. Segura, and A. Chevy, *Proceedings of the E.C. Photovoltaic Solar Energy Conference* (Reidel, Dordrecht, 1996), p. 2023.
- <sup>5</sup>P. Gomes da Costa, M. Balkanski, and R. F. Wallis, *Phys. Rev. B* **43**, 7066 (1991).
- <sup>6</sup>*Landolt-Börnstein Tables. III–VI Compounds*, edited by O. Madelung, New Series, Group III, Vol. 17f. (Springer Verlag, Berlin, 1983).
- <sup>7</sup>M. Julien-Pouzol, S. Jaulmes, M. Guittard, and F. Alapini, *Acta Crystallogr., Sect. B: Struct. Crystallogr. Cryst. Chem.* **B35**, 2848 (1979).
- <sup>8</sup>A. Linkforman, D. Carré, J. Etienne, and B. Bachet, *Acta Crystallogr., Sect. B: Struct. Crystallogr. Cryst. Chem.* **B31**, 1252 (1975).
- <sup>9</sup>J. Rigoult, A. Rimsky, and A. Kuhn, *Acta Crystallogr., Sect. B: Struct. Crystallogr. Cryst. Chem.* **B36**, 916 (1980).
- <sup>10</sup>A. R. Goñi, A. Cantarero, U. Schwarz, K. Syassen, and A. Chevy, *Phys. Rev. B* **45**, 4221 (1992).
- <sup>11</sup>D. Errandonea, F. J. Manjón, J. Pellicer, A. Segura, and V. Muñoz, *Phys. Status Solidi B* **211**, 33 (1999).
- <sup>12</sup>N. Kuroda, O. Ueno, and Y. Nishina, *J. Phys. Soc. Jpn.* **55**, 581 (1986).
- <sup>13</sup>F. J. Manjón, de Vijver, A. Segura, V. Muñoz, Z. Liu, and C. Ulrich, *Phys. Status Solidi B* **211**, 105 (1999).
- <sup>14</sup>D. Errandonea, A. Segura, V. Muñoz, and A. Chevy, *Phys. Status Solidi B* **211**, 201 (1999).
- <sup>15</sup>U. Schwarz, A. R. Goñi, K. Syassen, A. Cantarero, and A. Chevy, *High Press. Res.* **8**, 396 (1991).
- <sup>16</sup>D. Errandonea, A. Segura, J. F. Sánchez-Royo, V. Muñoz, P. Grima, A. Chevy, and C. Ulrich, *Phys. Rev. B* **55**, 16 217 (1997).
- <sup>17</sup>C. Ulrich, M. A. Mroginski, A. R. Goñi, A. Cantarero, U. Schwarz, V. Muñoz, and K. Syassen, *Phys. Status Solidi B* **198**, 121 (1996).
- <sup>18</sup>N. Kuroda, Y. Nishina, H. Iwasaki, and Y. Watanabe, *Solid State Commun.* **38**, 139 (1981).
- <sup>19</sup>H. Iwasaki, Y. Watanabe, N. Kuroda, and Y. Nishina, *Physics B* **105**, 314 (1981).
- <sup>20</sup>F. J. Manjón (private communication).
- <sup>21</sup>H. d'Amour, W. B. Holzapfel, A. Polian, and A. Chevy, *Solid State Commun.* **44**, 853 (1982).
- <sup>22</sup>C. Ulrich, Ph.D. thesis, Max-Planck-Institut für fesktörperforschung (Stuttgart), 1997.
- <sup>23</sup>D. C. Konigsberger and R. Prins, *X-ray Absorption: Principles, Applications, Techniques of EXAFS, SEXAFS and XANES* (Wiley Interscience, New York, 1988).
- <sup>24</sup>J. P. Itié, V. Briois, D. Martinez, A. Polian, and A. San Miguel, *Phys. Status Solidi B* **211**, 323 (1999).
- <sup>25</sup>A. San Miguel, A. Polian, and J. P. Itié, *Physica B* **208&209**, 117 (1995).
- <sup>26</sup>J. C. Chervin, B. Canny, J. M. Besson, and Ph. Pruzan, *Rev. Sci. Instrum.* **66**, 2595 (1995).
- <sup>27</sup>G. J. Piermarini and S. Block, *Rev. Sci. Instrum.* **46**, 973 (1975).
- <sup>28</sup>M. Hagelstein, A. San Miguel, A. Fontaine, and J. Goulon, *J. Phys. IV* **7**, 303 (1997).
- <sup>29</sup>J. Pellicer-Porres, A. San Miguel, and A. Fontaine, *J. Synchrotron Radiat.* **5**, 1250 (1998).
- <sup>30</sup>H. Tolentino, F. Baudalet, E. Dartyge, A. Fontaine, A. Lena, and G. Tourillon, *Nucl. Instrum. Methods Phys. Res. A* **286**, 307 (1990).
- <sup>31</sup>B. K. Teo and P. A. Lee, *J. Am. Chem. Soc.* **101**, 2815 (1979).
- <sup>32</sup>F. D. Murnaghan, *Proc. Natl. Acad. Sci. USA* **30**, 244 (1944).
- <sup>33</sup>J. P. Itié, A. Polian, M. Gauthier, and A. San Miguel, in *High-lights ESRF 96-97*, edited by ESRF Information Office (ESRF, Grenoble, 1997), p. 58,
- <sup>34</sup>J. Pellicer-Porres, A. Segura, A. San Miguel, and V. Muñoz, *Phys. Status Solidi B* **211**, 389 (1999).
- <sup>35</sup>J. Pellicer, F. J. Manjon, A. Segura, C. Power, J. Gonzalez, and V. Muñoz, *Phys. Rev. B* (to be published).
- <sup>36</sup>G. Kress and J. Hafner, *Phys. Rev. B* **47**, 558 (1993).
- <sup>37</sup>A. San Miguel, Ph.D. thesis, Université Paris VI, 1993.
- <sup>38</sup>A. San Miguel, A. Polian, M. Gauthier, and J. P. Itié, *Phys. Rev. B* **48**, 8683 (1993).
- <sup>39</sup>M. Gauthier, A. Polian, J. M. Besson, and A. Chevy, *Phys. Rev. B* **40**, 3837 (1989).
- <sup>40</sup>N. Kuroda, O. Ueno, and Y. Nishina, *Phys. Rev. B* **35**, 3860 (1987).